Environ. Sci. Technol. 2001, 35, 4189–4197

Emissions of Size-Segregated Aerosols from On-Road Vehicles in the Caldecott Tunnel

JONATHAN O. ALLEN,*,†,‡ PAUL R. MAYO,‡ LARA S. HUGHES,‡,§ LYNN G. SALMON,‡ AND GLEN R. CASS||

Environmental Engineering Science Department, California Institute of Technology, Pasadena, California 91125, and School of Earth and Atmospheric Science, Georgia Institute of Technology, Atlanta, Georgia 30332-0340

Particulate matter emissions from the California in-use vehicle fleet were measured as 37 500 vehicles traveled through two bores of the Caldecott Tunnel located in the San Francisco Bay area. Microorifice cascade impactors and filter-based samplers were used to determine the particle chemical composition as a function of particle size. Ammonia emissions from the vehicle fleet were measured as well. Concentrations of aerosol mass, organic carbon, elemental carbon, sulfate ion, nitrate ion, and ammonium ion, as well as 13 elements are reported. The particle mass distribution peaks in the particle size range 0.1–0.18 μm aerodynamic diameter (D_a). Elemental carbon and organic matter were the largest components of particle mass in all the size ranges studied. The Caldecott Tunnel bores studied include one which carries light-duty vehicle traffic and one which carries a mixture of light- and heavy-duty vehicle traffic. From experiments conducted in both bores, estimates are made of the size distribution and chemical composition of particulate matter emissions extrapolated to the 100% light-duty and 100% heavy-duty vehicle fleets. The heavy-duty vehicle fleet emitted 1285 ± 237 mg of fine particulate matter (D_a < 1.9 μm)/kg of C contained in the fuel burned (corresponding to approximately 430 ± 79 mg/km driven). Light-duty vehicles emitted less than 85 ± 6 mg/kg of C in the fuel burned (corresponding to less than approximately 5.5 ± 0.4 mg/km driven). Emissions of gas-phase ammonia in the Caldecott Tunnel were measured to be 194 and 267 mg/L of gasoline-equivalent fuel burned in the tunnel. The ammonia emissions are attributed to automobiles that were equipped with 3-way catalysts and operating fuel rich.

Introduction

Vehicle emissions make substantial contributions, both directly and indirectly, to atmospheric particle concentrations. Direct contributions include particulate emissions from tailpipes, brake lining wear, and tire wear. Indirect contributions include the emission of reactive gases, both organic and inorganic, which form secondary particulate matter via atmospheric transformations. In a recent estimate for the Los Angeles basin in September 1996, primary particles emitted from motor vehicles contributed 9–11% of the fine particle mass concentrations (*1*). Some compounds emitted by motor vehicles in the gas phase can contribute to aerosol mass when transformed by atmospheric chemical reactions. These gas-to-particle conversion products include nitrate, sulfate, and ammonium ions as well as organic matter. Gas-to-particle conversion products due to the emissions from all mobile plus stationary sources in the Los Angeles area contributed 37–65% of the fine particle mass during the 1996 case study referenced above; these products include transformed species originally emitted from motor vehicles as NO_x, SO_2, NH_3, and organic vapors. In addition, paved road dust reentrained into the atmosphere by vehicle traffic accounted for 5–10% of the atmospheric fine particle mass concentration during the 1996 study period.

Motor vehicle emission inventories normally used in air quality models are derived from tailpipe emissions measurements conducted on motor vehicles operated over simulated driving cycles on a chassis dynamometer. Source tests to determine the particulate matter size distribution and chemical composition are difficult and expensive to conduct; thus, the number of vehicles tested to date is relatively small. Further, conventional chassis dynamometer tests do not measure nontailpipe emissions such as those from tire and brake wear.

An alternative to single vehicle emissions measurements is to measure the emissions from a large population of on-road vehicles as they are driven through a highway tunnel. Particulate matter emissions measurements made in highway tunnels (*2–5*) are of particular interest for comparison with the results of this study. Over the years 1970–1979, Pierson and colleagues measured gaseous and particulate pollutant emissions in the Allegheny and Tuscarora Mountain Tunnels of the Pennsylvania Turnpike (*2*). They measured 35 analytes collected on filter samples and attributed emissions to either light-duty or heavy-duty vehicles. The particulate mass emission rate calculated for the heavy-duty vehicles observed during 10 studies in the period 1970–79 was 870 mg km^{-1}, compared to 25 mg km^{-1} for light-duty vehicles. The most important contributor to aerosol mass in these studies was carbonaceous particles from the heavy-duty trucks. In 1993, Weingartner et al. measured fine particle emissions in the Gubrist tunnel near Zurich, Switzerland (*3*). They measured fine particle mass emission rates of 383.5 mg km^{-1} for heavy-duty vehicles and 8.53 mg km^{-1} for light-duty vehicles. In 1993, Fraser, Cass, and Simoneit measured emissions in the Los Angeles area Van Nuys tunnel (*4*). The fine particle mass emission rate for a mixed vehicle fleet composed of 4% heavy-duty and 96% light-duty vehicles was 491 mg L^{-1} of fuel burned in the tunnel. This emission rate can be converted to 78 mg km^{-1} using those authors' estimated fleet-averaged fuel economy (*6*). The main components of fine particle mass in the Van Nuys tunnel were carbonaceous species and NH_4NO_3; the NH_4NO_3 was likely formed in the tunnel from the reaction of background HNO_3 with NH_3 emitted by the vehicles. In the summer of 1997, Kirchstetter et al. measured fine particle emissions in the Caldecott Tunnel, 4 months before the present study (*5*). Those authors calculated fine particle mass emission factors of 2.5 g kg^{-1} of fuel burned in the tunnel for heavy-duty diesel trucks and 0.11 g kg^{-1} for light-duty vehicles. Using the fuel and fleet fuel economy

* Corresponding author. Phone: (480) 965-4112; fax: (480) 965-0037; e-mail: joallen@asu.edu.

† Present address: Chemical & Materials Engineering and Civil & Environmental Engineering, Arizona State University, Tempe, AZ 82876-6006.

‡ Environmental Engineering Science Department.

§ Present address: Department of Chemistry, University of California, Riverside, CA, 92521.

|| School of Earth and Atmospheric Science.

10.1021/es0015545 CCC: $20.00
Published on Web 10/06/2001

data recommended by those authors, these emission factors are equivalent to 990 and 9.8 mg km^{-1} for heavy-duty diesel trucks and light-duty vehicles, respectively. Comparison between the 1997 Caldecott Tunnel and the 1970–79 Pennsylvania Turnpike tunnel experiments does not show the significant reduction in the emissions from heavy-duty diesel trucks that in fact has been achieved over the past 2 decades. This is due at least in part to the 4.2% upward sloping grade of the Caldecott Tunnel which is expected to increase emissions over those measured in the Pennsylvania Turnpike tunnels which have nearly level road beds. There are other differences between these two studies, but the 4.2% grade in the Caldecott Tunnel must be one of the major differences.

In the present work, we report size-segregated primary particle emission measurements made during November 1997 from the vehicle fleet traveling through the Caldecott Tunnel that connects Berkeley, CA, and Orinda, CA. The emissions from approximately 37500 vehicles were sampled during four experiments, each of 3-h duration. Measurements were made of fine particle (aerodynamic diameter, D_a, < 1.9 μm, $PM_{1.9}$) and PM_{10} (D_a < 10 μm) mass, carbonaceous particulate matter, inorganic ion, and metallic element concentrations in the tunnel and at a background site. From these concentration data, emission rates were calculated per kilogram of carbon consumed and per kilometer driven. Ammonia concentrations were also measured and ammonia emission rates were determined per liter of gasoline-equivalent fuel consumed. These measurements provide a complete set of size-segregated data on the chemical composition of fine particle emissions in a traffic tunnel. The Caldecott Tunnel is divided into separate bores, one which carries light-duty vehicle traffic and one which carries a mixture of light- and heavy-duty vehicles. From experiments conducted in both bores, estimates are made of emissions rates and particle chemical composition extrapolated to 100% light-duty and 100% heavy-duty vehicle fleets. We then compare these results with selected measurements made in other tunnel studies.

Experimental Methods

Sample Collection. The Caldecott Tunnel consists of three two-lane bores, running east–west between Berkeley, CA, and Orinda, CA, on a major commuting corridor into San Francisco. The tunnel is approximately 1.1 km long and slopes upward from west to east with a grade of approximately 4.2% (*7*). Ventilation shafts run the length of the tunnel bores. The tunnel bores are equipped with fans for forced ventilation; the fans were not operated during these experiments. Bore 1 carries mixed light-duty vehicle (LDV) and heavy-duty vehicle (HDV) traffic from west to east, and Bore 3 carries mixed vehicle traffic from east to west. Only LDVs are legally permitted to travel through Bore 2 in the direction of the prevailing flow of traffic, i.e., westward in the morning and eastward in the afternoon and evening. Thus, the eastbound traffic in the afternoon is driven uphill under load and is segregated by vehicle type in Bores 1 and 2, such that Bore 1 contains a mix of LDVs and HDVs, whereas Bore 2 contains almost exclusively LDVs plus a few stray HDVs that defy the rules (see Table 1). Since approximately 7% of the HDV traffic during the study actually uses the light-duty vehicle bore of the tunnel, we place "LDV Only" in quotes when referring to Bore 2 of the tunnel. The emissions from HDVs are much greater than those from LDVs, thus the stray HDVs in Bore 2 have an important influence on the results and interpretations of this study, and this is taken into account in the analysis of these data.

Pollutant concentrations in the tunnel bores were measured with a suite of sampling equipment positioned inside the ventilation shaft located directly above the roadway. Sampler inlets were inserted into the tunnel bores through slots in the floor of the ventilation shaft at a site approximately 50 m from the eastern exit of Bores 1 and 2. The equipment consisted of one filter sampler to collect PM_{10} samples, three fine particle filter samplers, and two cascade impactors. An identical suite of sampling equipment was operated concurrently at a background site in order to measure the outdoor pollutant concentrations. This site was located south of the East Fan house, approximately 400 m from the eastern exit of the tunnel.

TABLE 1. Caldecott Tunnel Sampling Events

			vehicle counts	
date	time (PST)	location	light duty	heavy duty
17 Nov 97	1200–1500	Bore 1	5657	342
18 Nov 97	1200–1500	Bore 1[a]	5978	436
19 Nov 97	1530–1830	Bore 2	12 681	30
20 Nov 97	1530–1830	Bore 2[b]	12 406	31

[a] Only fine particle filters operated at background site. [b] Only fine particle and PM_{10} filters operated at background site.

Particles were sampled from Bore 1 (containing both LDVs and HDVs) during the period of highest expected HDV traffic, from 1200 to 1500 h PST, on November 17 and 18, 1997 (see Table 1). Particles were sampled from Bore 2 of the tunnel ("LDV Only") during the period of highest expected LDV traffic, from 1530 to 1830 h PST, on November 19 and 20, 1997. Background air samplers were operated concurrently. Vehicles were counted by Prof. Deborah Niemeir's research group at the University of California, Davis.

The sampling equipment was identical to that used in the ambient aerosol sampling program of the 1997 Southern California Ozone Study and is fully described elsewhere (*8*); an abbreviated description of the equipment is presented here.

In the PM_{10} samplers, air was drawn at a rate of 16.7 L min^{-1} through an EPA-approved low volume PM_{10} inlet (Andersen Instruments, Smyrna, GA) and distributed between two parallel filter holders. A 47 mm diameter poly(tetrafluoroethylene) (PTFE) filter was used to collect particulate matter for gravimetric and inorganic species analyses. A 47 mm diameter prebaked quartz-fiber filter was used to collect particles for carbonaceous species analyses. In each of three fine particle samplers, ambient air was drawn at a nominal flow rate of 28 L min^{-1} through an acid-washed Pyrex glass inlet line. The air then passed through a PTFE-coated AIHL-design cyclone separator which removed particles with aerodynamic diameters larger than 1.9 μm (*9*). Following the cyclone, the airstream of one sampler was split in half and ducted to one PTFE filter and one quartz-fiber filter arranged in parallel. In the second fine particle sampler, the airstream was split in half and ducted to two quartz-fiber filters in parallel. A denuder difference system was used to measure gas-phase nitric acid concentrations in the third fine particle sampler; samples were collected on one PTFE filter at 14 L min^{-1} and two parallel nylon filters at 7 L min^{-1} each, one of which was downstream of a MgO coated tubular denuder (*10*). An open-faced filter stack also was operated at 10 L min^{-1} to collect gas-phase ammonia. This consisted of a PTFE filter to remove aerosol particles followed by two glass-fiber filters in series which had been impregnated with oxalic acid (*10*). The air flow rate across each filter was controlled by a critical orifice downstream of the filter. Actual flow rates were measured with a calibrated rotameter at the beginning and end of each sampling period.

Two cascade impactors were operated at each sampling site. These were 10 stage microorifice impactors (MOI) manufactured by MSP Corporation (Minneapolis, MN) (*11*). Each MOI was preceded by an AIHL-design cyclone separator which removed particles larger than 1.8 μm. Coarse particles

were removed by the cyclone separators because these larger particles may be more likely to bounce off their intended impaction stage and contaminate the fine particle samples. Ambient air was drawn through the impactor sampling systems at a nominal flow rate of 30 L min^{-1}. Pressures at impactor stages 5 and 10 were monitored and the flow rate controlled to maintain the pressure on these stages within the instrument design values. The actual flow rates through the impactors were subsequently determined from pressure drop measurements made across a calibrated orifice (MSP Corporation). To avoid sample contamination, no coatings were applied to the impaction substrates. Samples collected on impactor stages 5 though 10 and the afterfilter were analyzed; these stages have designed lower aerodynamic diameter, D_a, cutoffs of 1.0, 0.56, 0.32, 0.18, 0.1, and 0.056 μm. One MOI was equipped with PTFE impaction substrates (47 mm diameter, Gelman Teflo, 1.0 μm pore size) for gravimetric, ionic species, and elemental analysis. The other MOI was equipped with 47 mm diameter aluminum foil substrates (MSP Corporation) which were baked at 550 °C for at least 8 h. The aluminum foil substrates were used to collect samples for determination of mass, organic carbon, and elemental carbon.

Sample Analyses. Methods for chemical analysis of samples were identical to those used in the aerosol sampling program of the 1997 Southern California Ozone Study. These methods are fully described elsewhere (*8*); abbreviated descriptions of the analytical methods are presented here.

PTFE filters and impaction substrates were weighed before and after sampling using a mechanical microgram balance with a 1 μg sensitivity (Mettler Instruments, model M-5S-A) to determine aerosol mass concentrations gravimetrically. The filters and impaction substrates were equilibrated at 22.9 ± 0.3 °C and 48 ± 3% relative humidity for 24 h prior to weighing.

PTFE and oxalic acid coated glass-fiber filters were extracted into deionized water. The nylon filters were extracted in a buffer solution. Concentrations of the major ionic species, SO_4^{2-}, NO_3^-, and Cl^-, in the extracts were determined using a Dionex Model 2020i ion chromatograph. Filter extracts were also analyzed for the ammonium ion (NH_4^+) by an indophenol colorimetric procedure employing a rapid flow analyzer (Alpkem Corp., RFA-300 TM). Gas phase nitric acid concentrations were determined by the denuder difference method (*10*). Ammonia concentrations were determined from the extracts of oxalic acid-impregnated filters by the colorimetric procedure described previously for aerosol NH_4^+.

Elemental carbon (EC) and organic carbon (OC) concentrations in the aerosol samples were measured by a thermal-optical technique (*12, 13*). Prior to sample collection, these filters were heat treated at 550 °C in air for at least 8 h to lower their carbon blank levels. EC and OC analyses of aluminum impaction substrates were performed in a similar manner according to the procedures described by Kleeman et al. (*14*). The impaction media also were heat treated prior to use at 550 °C in air for 48 h. Organic matter concentrations reported throughout this work were estimated from measured OC concentrations by multiplying by a factor of 1.2 to account for the additional mass of associated H, O, N, and S present in particles emitted from vehicle tailpipes (*15*).

The concentrations of 36 major and minor trace elements were measured by instrumental neutron activation analysis (*16*). These elements are Al, As, Au, Ba, Br, Cd, Ce, Cl, Co, Cr, Cs, Eu, Fe, Ga, Hg, In, K, La, Lu, Mg, Mn, Mo, Na, Nd, Rb, Sb, Sc, Se, Sm, Sr, Th, Ti, U, V, Yb, and Zn. Of these 36 elements, 13 were found to have concentrations significantly different from zero in at least one tunnel sample (see Table 2).

All concentration values reported here have been blank corrected by subtracting the appropriate field blank concentrations, and the variances were estimated by adding the field blank and sample concentration variances.

Results and Discussion

Particle Concentrations. Particle mass concentrations measured inside Bore 1, in which both light-duty vehicle (LDV) and heavy-duty vehicle (HDV) traffic is permitted, were significantly higher than those measured in Bore 2, in which only LDVs were permitted. Particle mass concentrations in the tunnel bores were also significantly elevated relative to background concentrations in the outdoor air near the tunnel during all the sampling events. For example, the average $PM_{1.9}$ mass concentration was 102 $\mu g\ m^{-3}$ in Bore 1 (HDV and LDV) and 32 $\mu g\ m^{-3}$ in Bore 2 ("LDV Only"), while the average background $PM_{1.9}$ mass concentration was 7.1 $\mu g\ m^{-3}$. Particulate elemental carbon (EC) and organic matter concentrations measured inside the tunnel were also significantly elevated relative to background concentrations in all the samples. Concentrations of the inorganic ions NH_4^+, NO_3^-, and SO_4^{2-} were generally above background concentrations. Some of the metals measured here, particularly Al, Ba, Cr, Fe, Hg, La, Mg, Mn, Na, Sb, Sc, V, and Zn, were present in the tunnel at concentrations significantly greater than the background concentrations.

Vehicle emissions are proportional to the background-subtracted concentrations in each tunnel, hence particle concentration data presented hereafter are concentrations measured in the tunnels less the background concentrations. The original data are reported elsewhere (*8*). $PM_{1.9}$ background samples were collected every day of the study. PM_{10} samples were collected at the background site on 3 of the 4 days studied (see Table 1). Day-to-day variations in PM_{10} background concentrations were found to be significantly greater than analytical uncertainties, therefore PM_{10} data from the day when background samples were not collected are not included in the background-subtracted concentrations. Impactor samples were collected at the background site on 2 of the 4 study days. Fine particle background concentrations were found to be identical from day to day within analytical uncertainties; therefore, average background concentrations were subtracted from impactor data on days that background impactor samples were not collected. The reported uncertainties are one standard deviation calculated from the sum of the tunnel and background sample variances. Note that background-subtracted concentrations of aerosol mass, EC, organic matter, NH_4^+, NO_3^-, and SO_4^{2-} measured in the same tunnel bore on different days agree within experimental error.

Mass balances of the background-subtracted aerosol concentrations averaged over experiments in each tunnel show that the majority of the PM_{10} mass in the tunnel is carbonaceous (see Figure 1a). EC is the largest contributor to PM_{10} in Bore 1 (HDV and LDV) and organic matter is the largest contributor to PM_{10} in Bore 2 ("LDV Only"). Other important contributors to PM_{10} are NH_4^+, SO_4^{2-}, Fe, and Zn. In this and other mass balance figures, metals commonly found in crustal material are assumed to be present as oxides; these oxides are Al_2O_3, BaO, CrO_3, Fe_2O_3, HgO, Mn_2O_7, Sb_2O_5, V_2O_5, and ZnO. The majority of $PM_{1.9}$ also is carbonaceous (see Figure 1b); as was the case for PM_{10}, EC is the largest contributor to $PM_{1.9}$ in Bore 1 (HDV and LDV) and organic matter is the largest contributor in Bore 2 ("LDV Only"). Other important contributors to $PM_{1.9}$ are NH_4^+ and SO_4^{2-}.

The horizontal bars drawn across the results in Figure 1 show the gravimetrically determined mass concentrations which are different from the sum of the identified species. One source of this difference may be analytical uncertainty, which is often larger for the gravimetric mass measurements than for the chemical analyses. In one case, the gravimetrically

TABLE 2. PM_{10} and $PM_{1.9}$ Emissions Per Mass Carbon Consumed in the Caldecott Tunnel (mg kg of C^{-1})

	measured		calculated	
	Bore 1 (LDV and HDV)	Bore 2 ("LDV Only")	100% HDV	100% LDV
PM_{10} emissions				
mass	**603.0 ± 33.0**	**96.0 ± 12.0**	**2262.0 ± 156.0**	**68.0 ± 24.0**
organic matter	**212.0 ± 48.0**	**58.0 ± 17.0**	**714.4 ± 8.2**	**49.9 ± 1.3**
elemental carbon	**342.0 ± 31.0**	**56.0 ± 11.0**	**1278.0 ± 54.0**	**40.5 ± 8.3**
NH_4^+	**25.6 ± 1.3**	**12.45 ± 0.51**	**68.7 ± 3.8**	**11.74 ± 0.58**
NO_3^-	3.4 ± 5.5	1.4 ± 2.2	**10.0 ± 3.1**	**1.24 ± 0.48**
SO_4^{2-}	**14.8 ± 4.0**	2.4 ± 1.6	**55.5 ± 8.5**	1.7 ± 1.3
Al	3.5 ± 4.9	0.7 ± 1.8	**12.6 ± 2.0**	0.56 ± 0.30
Ba		**0.69 ± 0.16**		
Cr	**0.377 ± 0.068**	0.018 ± 0.021	**1.55 ± 0.54**	−0.001 ± 0.083
Fe		**6.3 ± 2.3**		
Hg	0.000 22 ± 0.000 94	**0.001 12 ± 0.000 39**		
La	0.0050 ± 0.0052	0.0016 ± 0.0020	**0.01608 ± 0.000 99**	**0.00141 ± 0.000 15**
Mg	1.8 ± 1.4	0.66 ± 0.50	**5.56 ± 0.20**	**0.600 ± 0.031**
Mn	0.20 ± 0.10	0.060 ± 0.040	**0.66 ± 0.19**	0.052 ± 0.029
Na	0.49 ± 0.66	**0.93 ± 0.21**	−0.9 ± 1.1	**0.95 ± 0.17**
Sb	**0.121 ± 0.018**	**0.0648 ± 0.0070**	0.30 ± 0.22	0.062 ± 0.033
Sc	0.000 39 ± 0.000 85	0.000 18 ± 0.000 31	**0.001 06 ± 0.000 35**	**0.000 172 ± 0.000 054**
V	0.007 ± 0.016	0.0047 ± 0.0059	**0.0158 ± 0.0040**	**0.004 60 ± 0.000 61**
Zn	**9.1 ± 2.5**	0.23 ± 0.89	**38.0 ± 10.**	−0.2 ± 1.6
$PM_{1.9}$ emissions				
mass	**394.0 ± 15.0**	**84.5 ± 6.2**	**1285.0 ± 237.0**	73.0 ± 51.0
organic matter	**160.0 ± 16.0**	**43.1 ± 5.9**	**495.0 ± 105.0**	39.0 ± 22.0
elemental carbon	**223.0 ± 12.0**	**19.7 ± 3.7**	**788.0 ± 332.0**	15.0 ± 71.0
NH_4^+	**3.64 ± 0.25**	**2.03 ± 0.15**	8.4 ± 8.0	2.0 ± 1.7
NO_3^-	**7.6 ± 1.1**	0.52 ± 0.67	**28.9 ± 2.6**	0.12 ± 0.56
SO_4^{2-}	**8.75 ± 0.78**	**1.21 ± 0.47**	**30.4 ± 6.3**	0.9 ± 1.3
Al	**1.35 ± 0.19**	−0.208 ± 0.099	5.2 ± 7.4	−0.2 ± 1.6
Ba	**0.520 ± 0.067**	−0.065 ± 0.032		
Cr	−0.139 ± 0.021	−0.0120 ± 0.0046	−0.518 ± 0.044	−0.0049 ± 0.0093
Fe	0.0 ± 1.1	**2.26 ± 0.31**	−7.1 ± 7.9	2.5 ± 2.0
Hg	**0.001 64 ± 0.000 32**	0.000 11 ± 0.000 12	0.0055 ± 0.0067	0.0001 ± 0.0014
La	**0.001 20 ± 0.000 35**	0.000 20 ± 0.000 14	0.0039 ± 0.0043	0.0002 ± 0.0011
Mg	**1.75 ± 0.69**	0.022 ± 0.094	**7.4 ± 2.0**	−0.07 ± 0.31
Mn	**0.0350 ± 0.0015**	−0.008 71 ± 0.000 94	0.12 ± 0.61	0.00 ± 0.16
Na	**0.43 ± 0.14**	**0.245 ± 0.061**	0.7 ± 3.0	0.28 ± 0.64
Sb	**0.0132 ± 0.0034**	**0.0185 ± 0.0019**	−0.009 ± 0.071	0.020 ± 0.015
Sc	**0.000 39 ± 0.000 13**	−0.000 020 ± 0.000 036	0.0015 ± 0.0014	−0.000 02 ± 0.000 30
V	**0.0035 ± 0.0011**	−0.000 75 ± 0.000 41	0.013 ± 0.026	−0.0005 ± 0.0055
Zn	**0.39 ± 0.19**	−0.068 ± 0.061	1.5 ± 1.9	−0.06 ± 0.41

determined mass concentration is greater than the sum of the identified species; the unidentified mass may be due to species which are not determined, the most important among these are Ca and Si, which are commonly present as calcium carbonates and silicon oxides in soil and road dust samples. Water retained in the samples at the weighing conditions (~48% RH) would also contribute to the unidentified mass.

As discussed below, substantial gas-phase NH_3 emissions were observed in the Caldecott Tunnel. The apparent emissions of aerosol NH_4^+ and NO_3^- likely result from the formation of secondary particulate matter within the tunnel from the reaction of gas-phase NH_3 and HNO_3. The presence of aerosol SO_4^{2-} in higher concentrations in Bore 1 demonstrates that HDVs emit primary sulfates.

The impactor samples also were analyzed to determine the size-resolved aerosol chemical composition (see Figure 2). Aerosol mass concentrations in both Bore 1 (HDV and LDV) and Bore 2 ("LDV Only") have peaks at 0.1−0.18 μm particle aerodynamic diameter. In Bore 1 (HDV and LDV), the peak is comparatively broader (0.056−0.56 μm) and composed mainly of EC with lesser amounts of organic matter; ammonium and sulfate ions are present in most of the size fractions. In Bore 2 ("LDV Only"), the peak is narrower and contains more organic matter than EC. Data shown in Figure 2 for the afterfilter sample (D_a < 0.56 μm) should be viewed with caution, since organic vapors may adsorb on the quartz-fiber afterfilter.

The sum of aerosol mass measured on the impactor stages is significantly lower than that collected on the fine particle filters. Comparisons of individual analytes demonstrated that the sum of EC, NO_3^-, SO_4^{2-}, and NH_4^+ on the impactor stages matched that on the fine particle filters. In contrast, the sum of organic matter on the impactor stages was approximately one-half of that on the fine particle filters. The filter organic matter measurement may be artificially high due to the sorption of gas-phase species on the quartz fiber filters; the impactor organic matter measurements may also be artificially low due to the volatilization of collected organics from impaction deposits during sampling. Another cause for this difference is that the quartz-fiber afterfilters, which collect particles smaller than 0.056 μm, could not be analyzed gravimetrically.

The distributions of aerosol mass with particle size observed in the Caldecott tunnel are similar to those recorded in recent dynamometer-based measurements of motor vehicle exhaust by Kleeman et al. (*17*). In both the tunnel and dynamometer-based measurements, the aerosol mass peaks at 0.1−0.18 μm particle aerodynamic diameter. More aerosol mass is observed in larger particle size fractions (D_a = 0.18−1.8 μm) in the tunnel measurements relative to the dynamometer-based measurements. Emissions of the additional particles in this size range may come from tailpipes of vehicle types not included in the sample of vehicles measured using the dynamometer or from nontailpipe

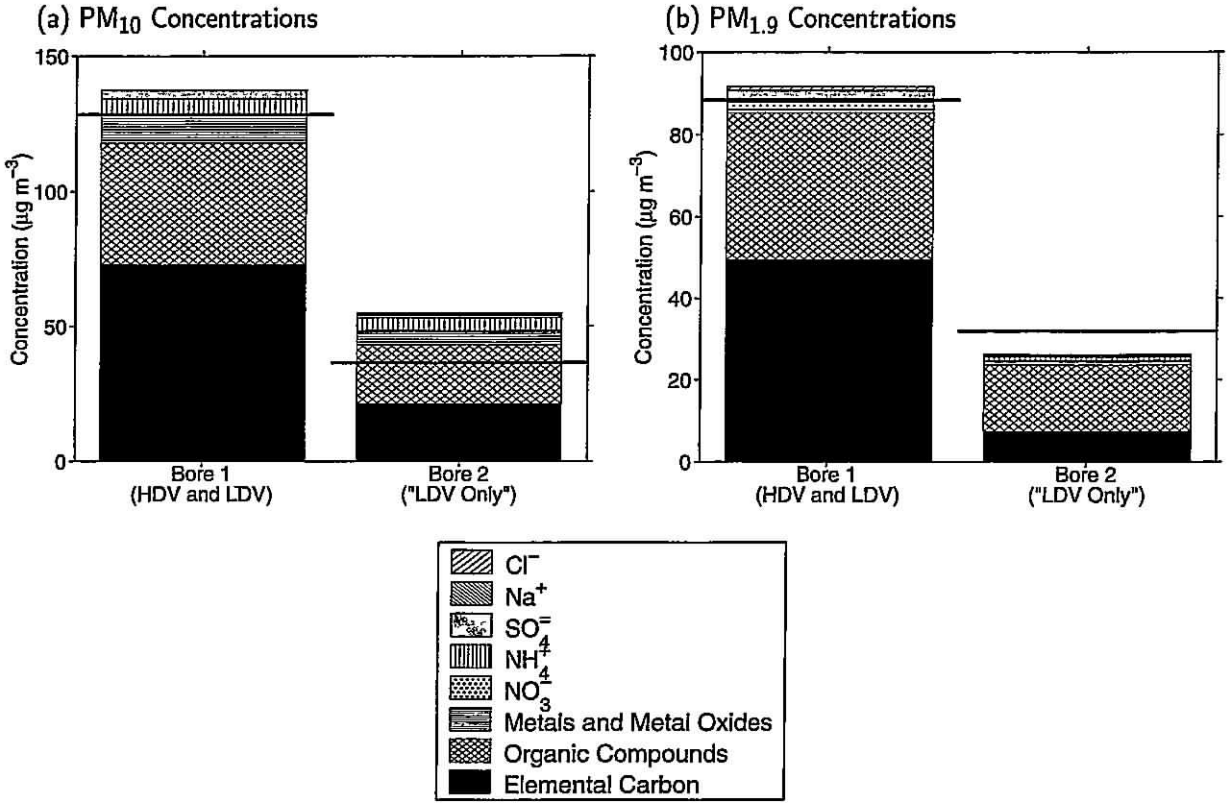

FIGURE 1. Mass balance on average PM_{10} and $PM_{1.9}$ concentrations in Bores 1 and 2 of the Caldecott Tunnel. The heavy horizontal lines show the gravimetrically measured mass concentrations.

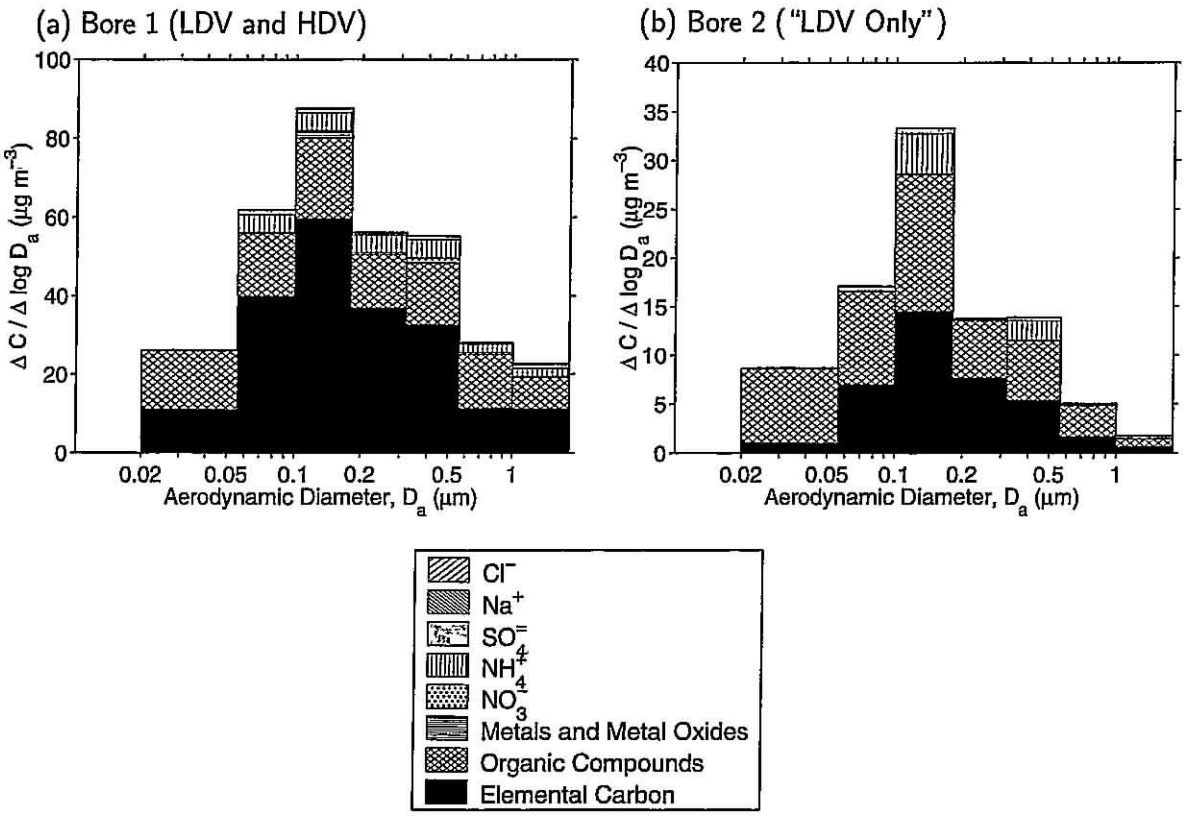

FIGURE 2. Size-segregated chemical composition of fine particles in Bores 1 and 2 of the Caldecott Tunnel.

emissions such as tire wear, road dust, and resuspended particulate emissions.

Thirteen metals were found to have concentrations significantly different from zero in at least one sample (see Table 2). The sources of these aerosol emissions can include a combination of tail-pipe emissions, nontail-pipe emissions, and resuspended road dust. Hildemann et al. have reported on the elemental composition of tail-pipe and nontail-pipe

emissions for automobiles and diesel-powered trucks (*18*). In that work Al, Fe, Mn, and Zn were found in tail-pipe emissions; Ba, Fe, Mn, and Zn were found in brake dust; those samples were not analyzed for Hg, La, Mg, Na, Sb, or Sc. Additional source tests should be conducted to identify the exact source(s) of the remaining metals.

Aerosol Emissions. Aerosol concentration measurements can be used to calculate emission rates from the vehicle fleet in the tunnel. The emission rate of species i per mass of carbon in the fuel burned, $E_{C,i}$, is a precise and directly measured emission rate. This is similar to emission rates stated as pollutant mass emitted per volume fuel burned as recommended by Singer and Harley (*19*). $E_{C,i}$ can be calculated from a material balance on the carbon in the fuel burned as

$$E_{C,i} = \frac{\Delta C_i}{\sum_j \Delta C_{C,j}} \quad (1)$$

where ΔC_i is the increase in concentration of species i between the tunnel interior and outdoor background, and $\Delta C_{C,j}$ is the increase in carbon concentration between the tunnel and background air due to species j. The increase in carbon concentration in the tunnel due to all species combined is a direct measure of fuel consumption and is calculated as

$$\sum_j \Delta C_{C,j} = \Delta[CO_2] + \Delta[CO] + \Delta[CH_4] + \Delta[NMHC] \quad (2)$$

where concentrations are expressed as carbon mass per unit air volume, and NMHC is the sum of carbon contained in gas-phase nonmethane hydrocarbons. Dr. Barbara Zielinska of the Desert Research Institute measured the concentrations of CO_2, CO, CH_4, and NMHC in the tunnel and background air during this study (*24*). Aerosol emissions contain less than 10^{-5} of the total carbon emissions; because these species make a negligible contribution to $\sum_j \Delta C_{C,j}$, they are not included in this summation.

The measured emission rates show that the majority of the aerosol emitted in the tunnel is carbonaceous with contributions from some metals (see Table 2). Emission rates which are significantly greater than zero are shown in bold in Table 2. The emission rates of most species are greater in the heavy-duty vehicle-influenced Bore 1 than in the "LDV only" Bore 2. Possible reasons for this are differences between the bores in (1) the proportion of HDVs, (2) the composition of the LDV fleet, and (3) driving conditions. Bore 1 was sampled in the early afternoon (1200–1500 h PST) while Bore 2 was sampled in the late afternoon (1530–1830 h PST) during the commuter rush. The LDV fleet driven in the early afternoon may include a higher proportion of older or poorly maintained cars than the commuter vehicle fleet driven home from work in the late afternoon. Driving conditions also differed between the early afternoon and late afternoon, when there was higher traffic density. Kirchstetter et al. measured vehicle speeds in the Caldecott Tunnel to be approximately 20 km h^{-1} faster in the early afternoon (1300–1500 h PDT) than during rush hour (1600–1800 h PDT) (*20*). In the same study, LDV CO emissions per unit fuel burned declined from 1300 to 1800 h PDT. We believe that the higher emission rates in Bore 1 are mostly due to the higher fraction of HDVs, although the different LDV fleet and higher average speeds in Bore 2 at different times of day may also have affected emissions.

Using the assumption that the differences in emission rates between Bores 1 and 2 are due entirely to the differences in the number of HDVs, one can estimate emission rates per mass of carbon burned for species i from the LDV fleet, $E_{C,i}$(LDV), and the HDV fleet, $E_{C,i}$(HDV). These estimates are derived from a linear regression analysis of the emission rates measured in each of the four experiments, j, as

$$E_{C,ij} = \phi_j E_{C,i}(\text{HDV}) + (1 - \phi_j) E_{C,i}(\text{LDV}) + \epsilon_{ij} \quad (3)$$

where $E_{C,ij}$ is the emission rate of species i from the entire vehicle fleet measured in experiment j, ϕ_j is the fraction of carbon emitted by HDVs in the tunnel during experiment j, and ϵ_{ij} is the residual difference between predicted and observed values. $E_{C,i}$(LDV) and $E_{C,i}$(HDV) were estimated using least squares linear regression.

The fraction of carbon emitted by the HDV fleet was estimated from vehicle counts and fleet-averaged fuel consumption estimates as

$$\phi = \frac{\sum_{\text{HDV}} n_k U_k \rho_k w_k}{\sum_{\text{All Vehicles}} n_k U_k \rho_k w_k} \quad (4)$$

where n_k is the number of vehicles of type k, U_k is the fuel consumption rate (L km^{-1}), ρ_k is the fuel density (kg L^{-1}), and w_k is the weight fraction carbon in the fuel.

For vehicle fleet calculations, the fleet was divided into four vehicle types: diesel-powered trucks with three or more axles, diesel-powered trucks with two axles and six tires, gasoline-powered trucks with two axles and six tires, and vehicles with two axles and four tires. Vehicles with three or more axles and those with two axles and six tires were considered HDVs here. This separation follows that of Kirchstetter et al. (*5*), who recorded vehicle types and determined the type of fuel used from license plate surveys. They report that 39% of the HDVs in Bore 1 had 3 or more axles while only 4% of the HDVs in Bore 2 had 3 or more axles. Kirchstetter et al. also surveyed vehicle license plates and estimated that >99% of vehicles with three or more axles were diesel powered and that 50% of vehicles with two axles and six tires were diesel powered. We use the distributions of vehicle type and fuel use reported by Kirchstetter et al. to estimate the diesel-powered vehicle population in the fleet sampled here. The number of vehicles in each type were calculated by scaling the relative distribution of vehicle types measured by Kirchstetter et al. to match the vehicle counts made for this study. Note that, based on California Air Resource Board motor vehicle emission inventory program (MVEI7G) (*21*), the LDV fleet in Contra Costa County, CA, includes 1% diesel-powered vehicles and 28% light duty trucks.

Fuel consumption rates used were those measured in the uphill section of the Fort McHenry tunnel for which Pierson et al. report fuel economies of 2.04 and 9.78 km L^{-1} for the HDV and LDV fleets, respectively (*22*). The uphill part of the Fort McHenry Tunnel has a 3.8% grade, similar to that for the Caldecott. Kirchstetter et al. sampled gasolines sold in the vicinity of the Caldecott Tunnel in 1997 (*20*). They report w to be 0.85 and ρ to be 0.74 g cm^{-3} for these California Phase II reformulated gasoline samples. For diesel fuel, we use 0.87 for w and 0.84 g cm^{-3} for ρ (*5*).

The calculated emission rates are presented in Table 2. The uncertainties shown for the calculated values represent 69% confidence intervals; this interval was chosen to be comparable with the one standard deviation confidence interval shown for the laboratory analytical results. The measured and extrapolated emission rates of aerosol mass show the expected strong influence of HDVs on emissions (see Figure 3); emission data for other analytes show similar scatter. The LDV extrapolated fleet emission rates are generally not greater than zero with 95% confidence.

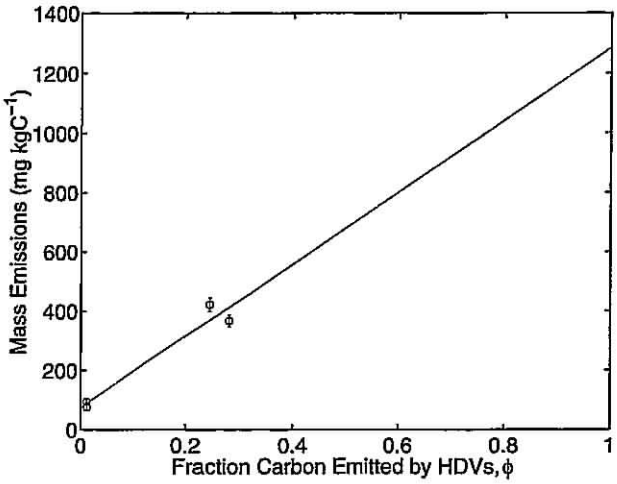

FIGURE 3. Fine particulate mass emissions (mg/kg of C burned in the fuel) plotted against fraction C emitted by heavy-duty vehicles (HDVs). Line shows linear regression to determine fine particulate mass emissions for the heavy-duty and light-duty vehicle fleets.

However, the Bore 2 emission rates generally agree with the 100% LDV fleet emission rate estimates and are more precise; these values can be used to place an upper limit on the LDV fleet emissions in place of the extrapolated values.

The majority of PM_{10} and $PM_{1.9}$ mass emitted by the HDV fleet is carbonaceous (see Figure 4). EC is the largest component and organic matter the second largest component of these emissions. Other significant contributors to PM_{10} and $PM_{1.9}$ emissions by the HDV fleet are NH_4^+, NO_3^-, SO_4^{2-}, Al, Cr, Mg, and Zn. Size-resolved aerosol emissions extrapolated to the condition of a 100% HDV fleet show a relatively broad peak (0.056–0.56 μm) which is composed mainly of EC with lesser amounts of organic matter; ammonium and sulfate ions are present in most of the size fractions (see Figure 5). The PM_{10} and $PM_{1.9}$ mass emitted by the LDV fleet is much smaller than that emitted by the HDV fleet; the bar graphs for the LDV fleet in Figure 4 have a vertical scale that is expanded by a factor of 10 relative to the scale of the HDV emissions graph. PM_{10} emissions per kilograms of carbon burned by the LDV fleet are approximately 30 times lower than for the HDV fleet when measured gravimetrically and approximately 20 times lower when measured as a sum of chemical analytes. LDV $PM_{1.9}$ emissions are not significantly different from zero with 95% confidence. In place of the LDV $PM_{1.9}$ emissions, the Bore 2 $PM_{1.9}$ emissions are plotted in Figure 4b. Bore 2 is the "LDV only" bore of the tunnel and thus emissions in Bore 2 place an upper limit on the LDV fleet emissions. The largest component of LDV fleet emissions is organic matter. Please note that much of the elemental carbon emissions in the "LDV only" bore probably comes from the few diesel trucks present in that tunnel bore (see Table 1).

It is convenient to convert emission rates stated on the basis of carbon burned, $E_{C,i}$, to emission rates stated on the basis of a fuel volume consumed or distance driven. Emissions of species i on a gasoline-equivalent fuel-volume basis, $E_{V,i}$ were calculated as

$$E_{V,i} = \rho w E_{C,i} \tag{5}$$

where ρ and w are values for gasoline. Emission rates per volume of gasoline-equivalent fuel burned in the Caldecott Tunnel extrapolated to 100% HDV and 100% LDV fleets are 1423 ± 98 mg L^{-1} PM_{10} and 809 ± 149 mg L^{-1} $PM_{1.9}$ for HDVs compared to 43 ± 15 mg L^{-1} PM_{10} and a closely comparable

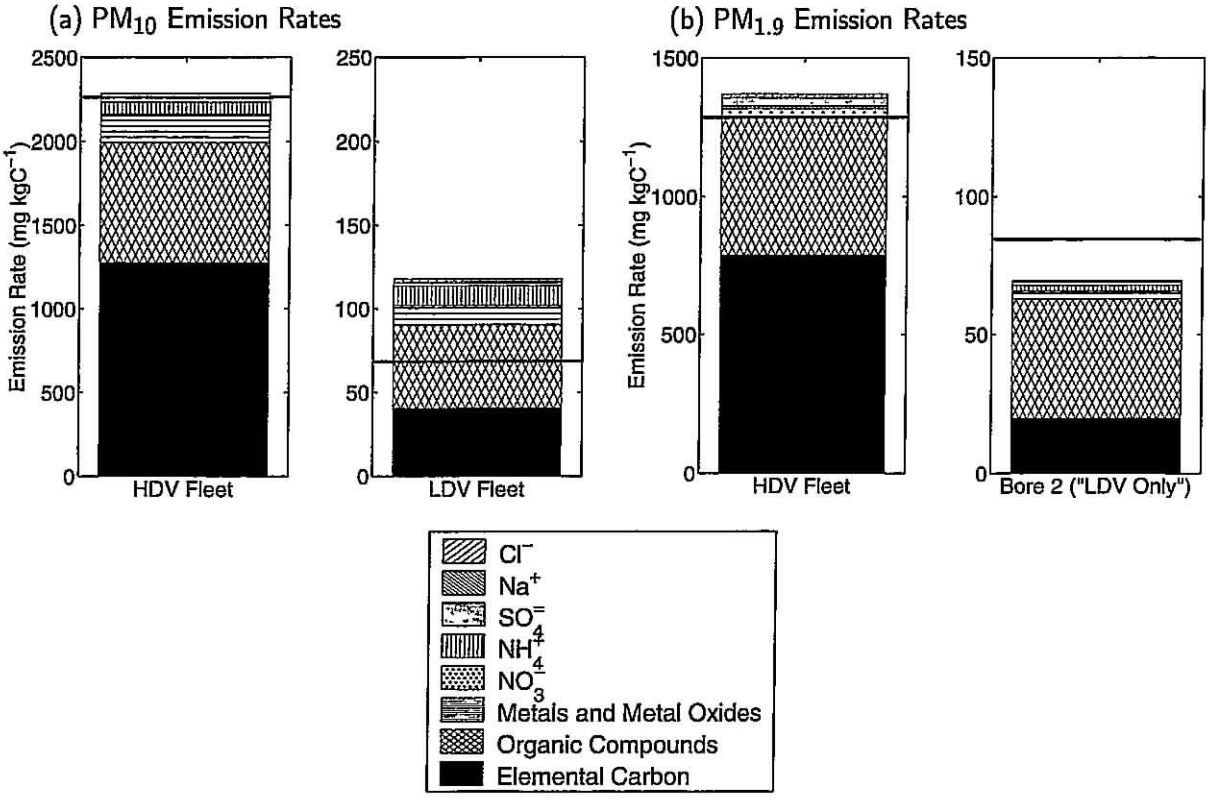

FIGURE 4. Calculated chemical composition of PM_{10} and $PM_{1.9}$ emissions for the heavy-duty vehicle (HDV) and light-duty vehicle (LDV) fleets (mg/kg of C burned in the fuel). The heavy horizontal lines show the gravimetrically determined mass emissions. Note the change in scale between the HDV and LDV plots. The $PM_{1.9}$ LDV data are based on the "LDV only" bore of the tunnel and act as an upper limit on LDV fleet emissions. Much of the elemental carbon seen in the "LDV only" bore probably comes from the few diesel trucks that use that tunnel bore without authorization (see Table 1).

TABLE 3. Gas-Phase Pollutant Concentrations in the Caldecott Tunnel

	Bore 1 (LDV and HDV)		Bore 2 ("LDV only")	
	17 Nov 97	18 Nov 97	19 Nov 97	20 Nov 97
CO_2 (ppmv)[a]	412.0 ± 14.0	459.0 ± 14.0	708.0 ± 13.0	769.0 ± 19.0
CO (ppmv)[a]	17.42 ± 0.66	19.22 ± 0.72	25.06 ± 0.65	26.71 ± 0.95
CH_4 (ppmv)[a]	0.16 ± 0.91	0.15 ± 0.91	0.23 ± 0.78	0.22 ± 0.91
NMHC (ppbC)[a]	1432.0 ± 16.0	1868.0 ± 21.0	2033.0 ± 16.0	2580.0 ± 28.0
HNO_3 ($\mu g\ m^{-3}$)	2.1 ± 1.1	0.80 ± 0.84	0.0 ± 1.0	−0.1 ± 1.0
NH_3 ($\mu g\ m^{-3}$)	99.1 ± 2.7	91.2 ± 2.3	100.2 ± 2.8	134.9 ± 2.8

[a] Measured by Dr. Barbara Zielinska of the Desert Research Institute (*24*).

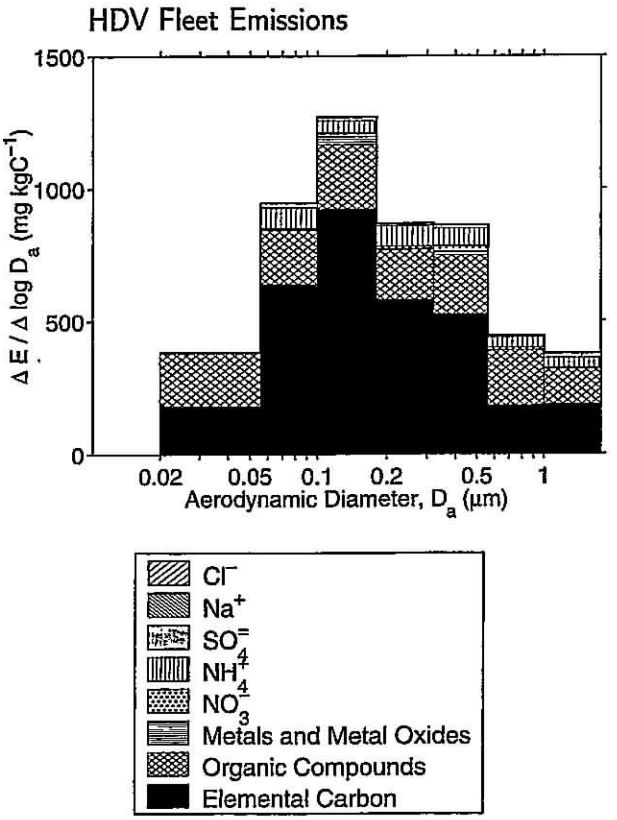

FIGURE 5. Calculated chemical composition of size-segregated aerosol emissions for the heavy-duty vehicle fleet (mg/kg of C burned in the fuel).

quantity of $PM_{1.9}$ for LDVs. Emission rates per unit fuel consumed (mg L^{-1}) can be obtained for other species by multiplying the emission rates (mg kg of C^{-1}) by 0.629.

Emissions of species i on a distance-driven basis, $E_{D,i}$ were calculated as

$$E_{D,i} = \overline{U\rho w} E_{C,i} \quad (6)$$

where $\overline{U\rho w}$ is the product of the fuel consumption rate, density, and carbon content averaged across vehicle types weighted by distance traveled by vehicles of each type, calculated as

$$\overline{U\rho w} = \frac{\sum n_k U_k \rho_k w_k}{\sum n_k} \quad (7)$$

Emission rates per distance driven in the Caldecott Tunnel extrapolated to 100% HDV and 100% LDV fleets are 756 ± 52 mg km^{-1} PM_{10} and 430 ± 79 mg km^{-1} $PM_{1.9}$ for HDVs compared to 4.4 ± 1.6 mg km^{-1} PM_{10} and a closely comparable quantity of $PM_{1.9}$ for LDVs. Emission rates per distance driven (mg km^{-1}) can be obtained for other species by multiplying the emission rates (mg kg of C^{-1}) by 0.334 and 0.065 for the 100% HDV and 100% LDV fleets, respectively. Note that the emission rates given (mg km^{-1}) represent the particular driving conditions in the Caldecott Tunnel; specifically, the emissions from warm vehicles driving at steady highway speeds up a fairly steep grade.

Emission rates also can be extrapolated to a fleet of 100% heavy-duty diesel-powered vehicles versus all other vehicles. The fraction of carbon emitted by heavy-duty diesel-powered vehicles was calculated from an equation analogous to eq 4 and the emissions data regressed using an equation analogous to eq 3. Emission rates for a fleet composed of 100% heavy-duty diesel powered vehicles were approximately 35% greater than those calculated for HDVs of all types (*8*). The relative chemical composition of emissions estimated for a fleet composed of 100% heavy-duty diesel powered vehicles was approximately the same as that shown for the overall HDV fleet in Figures 4 and 5.

Comparison to Aerosol Emissions Measured in Other Studies. Pierson et al. report estimated gasoline- and diesel-powered vehicle emissions on a milligram per kilometer traveled basis from measurements made in 1977 in the Tuscarora Mountain Tunnel (*2*). A comparison of these data with PM_{10} measurements from the present study show that mass emissions are approximately the same for heavy-duty diesel-powered vehicles, 865 mg km^{-1} in the Tuscarora Tunnel, and 1098 ± 79 mg km^{-1} in the present study. Particulate matter emission rates for light-duty vehicles, in contrast, have been reduced substantially between 1977 and 1997, declining from 51 mg km^{-1} in the Tuscarora Tunnel to less than 5 mg km^{-1} in the Caldecott Tunnel. This is due in part to the removal of lead from gasoline. These reductions in light-duty vehicle emissions are observed even though the Caldecott tunnel has a 4.2% grade and the Tuscarora Mountain Tunnel is essentially flat.

Weingartner et al. report fine particulate matter emissions (D_a < 3.0 μm) in the Gubrist Tunnel near Zurich, Switzerland (*3*) to be 383.5 mg km^{-1} for heavy-duty vehicles, and 8.53 mg km^{-1} for light-duty vehicles. These HDV fine particle mass emission factors are equal within experimental uncertainty to those measured here for $PM_{1.9}$, 429 ± 79 mg km^{-1}. The fine particle emissions from the LDV fleet measured here (4.7 ± 3.3 mg km^{-1}) likewise are statistically indistinguishable from the Gubrist Tunnel results at the 95% confidence level.

Emissions from a mixed fleet of heavy- and light-duty vehicles were measured by Fraser et al. in the Los Angeles area Van Nuys tunnel in 1993 (*4*); these are most closely comparable with emission rates in the mixed vehicle Bore 1 of the Caldecott Tunnel. Fine particle mass emission rates in the Van Nuys tunnel were 491 mg L^{-1}. This is substantially greater than the $PM_{1.9}$ emission rates reported here for Bore 1 (248 ± 9 mg L^{-1}). Fine EC and OC emission factors are equivalent between these two studies within experimental error. Higher "emissions" of NO_3^- and NH_4^+ were observed in the Van Nuys tunnel; these "emissions" likely result from

the formation of secondary particulate matter within the tunnel from the reaction of gas-phase NH_3 and HNO_3. Therefore, the mass emission factors agree with the exception that a greater quantity of secondary aerosol, primarily NH_4NO_3, was formed in the Van Nuys tunnel as compared to the Caldecott Tunnel.

Kirchstetter et al. report emissions of fine ($D_a < 2.5\ \mu m$) particulate matter to be 1850 ± 148 and 81.4 ± 7.4 mg L^{-1} for heavy-duty diesel trucks and other vehicles on a gasoline-equivalent fuel basis (*5*). These measurements were made in the Caldecott Tunnel in the summer of 1997, 4 months before the present study. Their estimates for the heavy-duty diesel trucks are significantly higher than the $PM_{1.9}$ emissions reported here (1089 ± 210 mg L^{-1}). Background-subtracted fine particle mass concentrations within the Caldecott Tunnel reported by Kirchstetter et al. were 31% greater than those reported for Bore 1 and 26% higher for Bore 2 than in the present study. Similarly, the fine particle EC and OC emission rates estimated by Kirchstetter et al. are significantly higher than the $PM_{1.9}$ emissions reported here. Since traffic densities during the two studies were comparable, this comparison suggests that a systematic difference in measurement techniques led to higher concentration values in the Kirchstetter et al. study. One systematic difference was that Kirchstetter et al. collected $PM_{2.5}$, not $PM_{1.9}$. Comparison of PM_{10} data to $PM_{1.9}$ data from the present study shows a large quantity of particulate matter present in particles between 1.9 and 10 μm aerodynamic diameter due to the heavy-duty diesel trucks; a portion of these emissions are expected to be in the 1.9 to 2.5 μm size range.

Gas-Phase Emissions. Concentrations of ammonia in the gas phase within the Caldecott Tunnel substantially exceeded those in the outdoor air during all the sampling events. The average NH_3 concentrations before background subtraction were 103, 124, and 7 $\mu g\ m^{-3}$ in Bore 1 (LDV and HDV), Bore 2 ("LDV Only"), and at the outdoor background site, respectively. The background-subtracted gas concentrations are presented in Table 3. These observations confirm the findings of an experiment in the Los Angeles area Van Nuys Tunnel by Fraser and Cass that the in-use vehicle fleet emits substantial amounts of ammonia (*6*). The average emission rates of NH_3 were 267 and 194 mg L^{-1} of gasoline-equivalent fuel burned in Bores 1 and 2, respectively. Extrapolation of these data yield ammonia emission estimates of 467 ± 176 and 193 ± 38 mg L^{-1} for the 100% HDV and 100% LDV fleets, respectively. Note that the uncertainty of the HDV emission rate is relatively large. The ammonia emissions most likely are due to 3-way catalyst-equipped autos and light trucks that are running rich either because they are running under load or are poorly maintained (*6*, *23*).

The NH_3 emission rates of 194 and 267 mg L^{-1} observed in the Caldecott Tunnel are slightly lower than the 380 mg L^{-1} measured in 1993 the Los Angeles area Van Nuys Tunnel (*6*). In addition to increased gas-phase NH_3, Fraser and Cass reported apparent emission rates of 21.0 mg L^{-1} for aerosol NH_4^+, and 61.9 mg L^{-1} for aerosol NO_3^- in the Van Nuys Tunnel. These "emissions" likely result from the formation of secondary particulate matter within the tunnel from the reaction of gas-phase NH_3 and HNO_3. Thus, when the aerosol plus gas-phase data are combined, the total NH_3 emission rate in the Van Nuys Tunnel in 1993 was 400 mg L^{-1}. In contrast to the Caldecott Tunnel, the Van Nuys Tunnel is more nearly flat and traffic runs more slowly, suggesting that increased load on the engines is not a cause of the higher NH_3 emissions in the Van Nuys Tunnel. Thus, the higher emissions of NH_3, CO, and NMHC measured in the Van Nuys Tunnel are likely due to an older and possibly more poorly maintained vehicle fleet at that location when compared to the long distance commuter fleet that uses the Caldecott Tunnel.

Acknowledgments

This project was supported by the Coordinating Research Council, Inc., and the U.S. DOE Office of Heavy Vehicle Technologies through the National Renewable Energy Laboratory under CRC Project No. A-22. Thanks are due to CalTrans and the Caldecott Tunnel staff. VOC canister analyses were performed by Dr. Barbara Zielinska of the Desert Research Institute. Traffic counts were performed by Prof. Deborah Niemeir's research group at the University of California, Davis. INAA analyses were performed by Dr. Michael Ames and Dr. Jec Gone at the Nuclear Reactor Laboratory, Massachusetts Institute of Technology.

Literature Cited

(1) Kleeman, M. J.; Hughes, L. S.; Allen, J. O.; Cass, G. R. *Environ. Sci. Technol.* **1999**, *33*, 4331–4341.
(2) Pierson, W. R.; Brachaczek, W. W. *Aerosol Sci. Technol.* **1983**, *2*, 1–40.
(3) Weingartner, E.; Keller, C.; Stahel, W. A.; Burtscher, H.; Baltensperger, U. *Atmos. Environ.* **1997**, *31*, 451–462.
(4) Fraser, M. P.; Cass, G. R.; Simoneit, B. R. T. *Environ. Sci. Technol.* **1998**, *32*, 2051–2060.
(5) Kirchstetter, T. W.; Harley, R. A.; Kreisberg, N. M.; Stolzenburg, M. R.; Hering, S. V. *Atmos. Environ.* **1999**, *33*, 2955–2968.
(6) Fraser, M. P.; Cass, G. R. *Environ. Sci. Technol.* **1998**, *32*, 1053–1057.
(7) Kirchstetter, T. W.; Singer, B. C.; Harley, R. A.; Kendall, G. R.; Chan, W. *Environ. Sci. Technol.* **1996**, *30*, 661–670.
(8) Allen, J. O.; Hughes, L. S.; Salmon, L. G.; Mayo, P. R.; Johnson, R. J.; Cass, G. R., *Characterization and evolution of primary and secondary aerosols during $PM_{2.5}$ and PM_{10} episodes in the South Coast Air Basin*; Technical report, California Institute of Technology, Coordinating Research Council Project A-22, 2000.
(9) John, W.; Reischl, G. *J. Air Pollut. Control Assoc.* **1980**, *30*, 872–876.
(10) Solomon, P. A.; Larson, S. M.; Fall, T.; Cass, G. R. *Atmos. Environ.* **1988**, *22*, 1587–1594.
(11) Marple, V. A.; Rubow, K. L.; Behm, S. M. *Aerosol Sci. Technol.* **1991**, *14*, 434–446.
(12) Huntzicker, J. J.; Johnson, R. L.; Shah, J. J.; Cary, R. A., In *Particulate Carbon, Atmospheric Life Cycle*; Wolff, G. T., Klimisch, R. L., Eds.; Plenum: New York, 1982; pp 79–88.
(13) Birch, M. E.; Cary, R. A. *Aerosol Sci. Technol.* **1996**, *25*, 221–241.
(14) Kleeman, M. J.; Schauer, J. J.; Cass, G. R. *Environ. Sci. Technol.* **1999**, *33*, 3516–3523.
(15) Schauer, J. J.; Kleeman, M. J.; Cass, G. R.; Simoneit, B. R. T. *Environ. Sci. Technol.* **1999**, *33*, 1578–1587.
(16) Olmez, I. In *Methods of Air Sampling and Analysis*; Lodge, J. P., Jr., Ed.; Lewis Publishers: Chelsea, MI, 1989; 3rd ed., pp 143–150.
(17) Kleeman, M. J.; Schauer, J. J.; Cass, G. R. *Environ. Sci. Technol.* **2000**, *34*, 1132–1142.
(18) Hildemann, L. M.; Markowski, G. R.; Cass, G. R. *Environ. Sci. Technol.* **1991**, *25*, 744–759.
(19) Singer, B. C.; Harley, R. A. *J. Air Waste Manage. Assoc.* **1996**, *46*, 581–593.
(20) Kirchstetter, T. W.; Singer, B. C.; Harley, R. A.; Kendall, G. R.; Traverse, M. *Environ. Sci. Technol.* **1999**, *33*, 318–328.
(21) California Air Resources Board. *Methodology for estimating emissions from on-road motor vehicles*; Mobile Source Emission Inventory Branch, Sacramento, CA, November 1996.
(22) Pierson, W. R.; Gertler, A. W.; Robinson, N. F.; Sagebiel, J. C.; Zielinska, B.; Bishop, G. A.; Stedman, D. H.; Zweidinger, R. B.; Ray, W. D. *Atmos. Environ.* **1996**, *30*, 2233–2256.
(23) Cadle, S. H.; Mulawa, P. A. *Environ. Sci. Technol.* **1980**, *14*, 718–723.
(24) Zielinska, B.; Sagebiel, J.; Harshfield, G.; Fujita, E. *Air Monitoring Program for Determination of the Impacts of the Introduction of California's Phase 2 Reformulated Gasoline on Ambient Air Quality in the South Coast Air Basin*, Desert Research Institute, 1999.

Received for review August 3, 2000. Revised manuscript received June 27, 2001. Accepted June 27, 2001.

ES0015545